Environmental Science and Pollution Research (2018) 25:9887–9895
https://doi.org/10.1007/s11356-018-1298-6

RESEARCH ARTICLE

# Preparation and characterization of $Na_2S$-modified biochar for nickel removal

Xiaolan Hu[1] · Yingwen Xue[1] · Lina Liu[2] · Yifan Zeng[1] · Li Long[1]

Received: 6 October 2017 / Accepted: 15 January 2018 / Published online: 26 January 2018


## Abstract

Biochar has good adsorption ability to various contaminants. In this work, peanut shell, corncob, cotton stalks, and crayfish shell were pyrolyzed under three temperatures (300, 450, 600 °C) to obtain biochars for the removal of $Ni^{2+}$. The biochars were further modified with 2 mol/L $Na_2S$ solution. Characterization results showed that the specific surface area and total pore volume of the modified biochars increased substantially. Among all the adsorbents, the modified corncob biochar (450 °C) showed the best $Ni^{2+}$ adsorption. The adsorption kinetics followed the Elovich model with an equilibrium time of 24 h. The maximum capacity of the modified biochar reached 15.40 mg/g. The adsorption process was affected by pH, temperature, and coexisting ions. Increasing pH (under 7) provided more adsorption sites which enhanced adsorption capacity. Experimental results also indicated that the main adsorption mechanism of $Ni^{2+}$ was ion exchange. Findings from this work suggest that modified biochar can be used as an effective adsorbent for the removal of $Ni^{2+}$ from wastewater.

**Keywords** Biochar · $Ni^{2+}$ · Modification · Adsorption mechanism

## Introduction

The rapid development of the electronics industry has caused a large amount of wastewater containing nickel ($Ni^{2+}$) which has been discharged into the natural water bodies and municipal pipe network systems. The harm of nickel to the human body includes causing inflammation, inducing cancer (Gupta et al. 2003), affecting liver (Akhtar et al. 2004) and renal function (Villaescusa et al. 2004), and leading to neurasthenia. Nickel also has a destructive effect on many human bioenzymes by weakening their activity (Shukla et al. 2005). Because of the seriousness of nickel pollution, many scholars have conducted researches on the treatment of nickel-containing wastewater. Current treatment methods of nickel in wastewater include chemical precipitation, extraction, ion exchange (Christensen and Delwiche 1982), membrane separation, etc. Electrocoagulation (EC) is used in the removal of nickel from aqueous solutions, and the optimum removal efficiencies at nickel concentrations can reach 500 mg/L (Mansoorian et al. 2012). The ion exchange method is often used to remove $Ni^{2+}$ with good removal effect, but the process may cost more than other methods due to the regeneration requirement (Alyüz and Veli 2009; Ismail et al. 2014). Most of the chemical treatment methods have secondary contamination issues, which may add further burden on the environment (Sandau et al. 2010).

As a new adsorption material, biochar has attracted great research attention for its low cost and it is environmentally friendly (Mohan et al. 2014). The adsorption method is often used to remove contaminants from wastewater. At present, the most common low-cost adsorbents used in the adsorption removal method include ceramic (Rosengren et al. 2002), silica gel (Wang et al. 2005), zeolite (Alvarez-Ayuso et al. 2003), bentonite (Banerjee et al. 2003), kaolinite (Yavuz et al. 2003), corncob (Vaughan et al. 2001), etc. In previous studies, hydrothermal biochar made of pine and rice husk by Liu and Zhang (2009) and pyrogenic biochar of waste products and sugar beet

**Highlights** a. A new modification method is used in this paper.
b. The maximum adsorption capacity of $Ni^{2+}$ was 15.40 mg/g.
c. The adsorption mechanism was studied by using various characterizations.

Responsible editor: Guilherme L. Dotto

✉ Yingwen Xue
ywxue@whu.edu.cn

[1] School of Civil Engineering, Wuhan University, Wuhan, China

[2] College of Environmental Science and Engineering, Tongji University, Shanghai, China

by Doumer et al. (2016) have been used to remove $Ni^{2+}$, $Cd^{2+}$, $Pb^{2+}$, $Cu^{2+}$, and other heavy metal ions from aqueous solution.

Corncob biochars have been synthesized for treating wastewater containing metal ions, which were modified with either 0.6 M citric acid or 1.0 M phosphoric acid to help improve natural adsorption capacity (Vaughan et al. 2001). Ding et al. (2016) found that biochar modified by NaOH showed a much higher sorption effect of heavy metal ions (i.e., $Pb^{2+}$, $Cd^{2+}$, $Cu^{2+}$, $Zn^{2+}$, and $Ni^{2+}$) than the unmodified one in both single-metal and mixed-metal systems. This work showed that alkali modification greatly increased the surface area, oxygen-containing surface functional groups, which showed much higher sorption of heavy metal ions. Another research studied the adsorption of three metal ions (Hg(II), Pb(II), and Ni(II)) onto carbon aerogel (Goel et al. 2005). The adsorption mechanism was ion exchange between metal cations and $H^+$ at the carbon aerogel surface, especially carboxylic groups. All these treatments change the surface characteristics of the biochars and thus greatly enhance their adsorption ability to metal ions in aqueous solutions.

Hydroponic experiments were carried out to evaluate the ability of biochar filters to reduce the toxic effect of $Ni^{2+}$ on tomato growth (Mosa et al. 2016). Kobya et al. (2005) used activated carbon produced from apricot stone to adsorb heavy metals, and reported that its adsorption capacity of $Ni^{2+}$ reached 27.21 mg/g when pH was 6. The effect of the feedstock type was more obvious than the pyrolysis temperature on biochar's ability to remove nickel (Higashikawa et al. 2016). This makes biochars more multifunctional for environmental applications. The above experimental results indicate that biochar has huge potential to be used as alternative adsorbent for the removal of heavy metal pollutants from wastewater.

The specific objectives of this work were to (1) measure the sorption kinetics and isotherms of $Ni^{2+}$ onto modified biochar; (2) determine the effect of pH, temperature, and coexisting ions on the adsorption of nickel; and (3) explore adsorption mechanisms.

**Table 1** The $Ni^{2+}$ adsorption capacities of the biochars

| Raw materials | Adsorption capacity (mg/g) |
|---|---|
| PS300 | 4.92 ± 0.39 |
| PS450 | 3.54 ± 0.09 |
| PS600 | 4.90 ± 0.65 |
| CS300 | 5.57 ± 1.38 |
| CS450 | 5.87 ± 0.31 |
| CS600 | 5.65 ± 0.69 |
| CC300 | 1.39 ± 0.08 |
| CC450 | 7.85 ± 0.34 |
| CC600 | 3.84 ± 0.12 |
| CFS300 | 1.05 ± 0.12 |
| CFS450 | 1.71 ± 0.16 |
| CFS600 | 2.03 ± 0.02 |

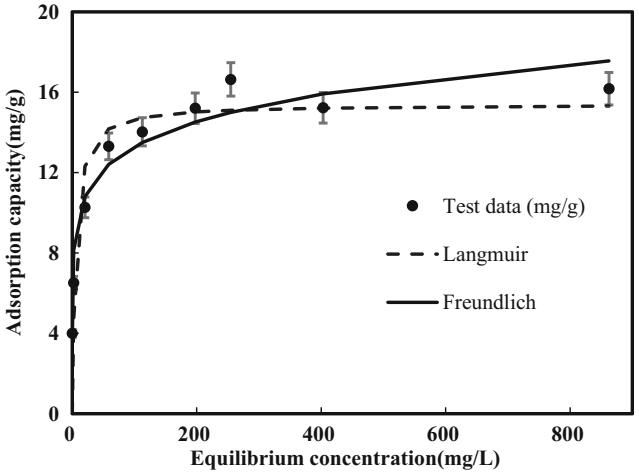


**Fig. 1** Adsorption isotherm of MCC450 to nickel. Symbols are means of triplicated data points, and error bars are the standard deviations

## Materials and methods

### Biochar production and modification

The biochars were produced from peanut shells (PS), cotton stalks (CS), corncobs (CC), and crayfish shell (CFS). Each of the feedstock materials was put in a tube furnace and pyrolyzed at a temperature of 300, 450, or 600 °C for 2 h. All of the resultant biochars were chilled and ground to a size range of 0.9~1.2 mm. After rinsing with deionized (DI) water, the samples were oven dried at 80 °C. To label the samples, biochar prepared from CC at 450 °C was labeled as CC450 (i.e., feedstock plus pyrolysis temperature), and the rest were oven dried using the same labeling method. A pre-experiment was conducted to select biochar with the best adsorption of $Ni^{2+}$ from the 12 samples. The selected biochar was then modified with 2.0 mol/L $Na_2S$ solution at a ratio of 1 g to 10 mL (Xu and Zhao 2007) for 2 h.

### Characterizations

The output of biochar was calculated by the weight of dry solid before and after pyrolysis. In order to thoroughly

**Table 2** Isothermal model parameters of Ni adsorption on MCC450

| Adsorbent | Langmuir | | | Freundlich | | |
|---|---|---|---|---|---|---|
| | $Q_{max}$ (mg/g) | $K$ | $R^2$ | $K_f$ | $n$ | $R^2$ |
| MCC450 | 15.40 | 0.197 | 0.83 | 7.33 | 0.13 | 0.94 |

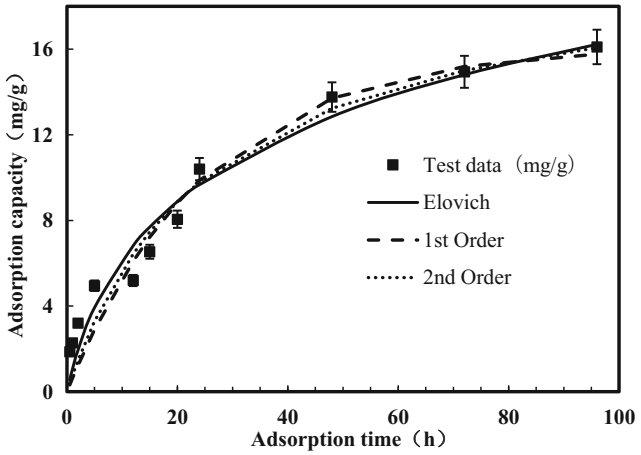


**Fig. 2** Adsorption kinetics of MCC450 to nickel. Symbols are means of triplicated data points, and error bars are the standard deviations

understand the adsorption mechanism, the modified biochar, which possessed the best adsorption effect, was characterized by different methods. A full automatic specific surface and aperture distribution analyzer (Mike Murray Feldman Instrument Co., Ltd., ASAP 2020 physical adsorption instrument) was used to measure the BET surface area, pore surface, and pore volume of the samples before and after adsorption. The species and characters of the functional groups on the surface of biochar before and after modification were analyzed by Fourier transform infrared spectroscopy (FTIR) (Nicolet 6700, Thermo Nicolet Company, USA). Surface elemental composition and elemental species were analyzed by X-ray photoelectron spectrometry (XPS) (Thermo Fisher Company, ESCALAB 250Xi).

### Batch adsorption experiment

The adsorption of $Ni^{2+}$ onto the biochar was measured by batch experiments. Every result came from at least three parallel samples. The initial $Ni^{2+}$ solution concentration was 50 mg/L. For each test, 50 mL $Ni^{2+}$ solution and 0.1 g biochar were mixed in a 50-mL centrifugal tube (Long et al. 2017). In order to ensure adequate contact in the progress of adsorption, the tube was positioned horizontally on the shaking table, shaking at 150 r/min.

A pre-experiment was carried at room temperature (25 ± 1 °C) for 24 h. The biochar and solution were separated by vacuum filtration using a 0.22-μm microporous membrane. The concentration of $Ni^{2+}$ in solution was then measured with the dimethylglyoxime spectrophotometric method. Based on the pre-experiment, the biochar with the highest sorption of $Ni^{2+}$ was modified to continue the batch experiment.

Three influence factors including temperature, solution pH, and coexisting ions were evaluated. The effect of temperature was determined by setting a series of temperature values (10, 20, 30, 40, and 50 °C). The effect of pH was tested by setting the solution pH to five values (pH = 1.8, 2.6, 5.0, 6.0, and 7.0). Pre-experiments had shown that precipitation occurred when the solution pH was higher than 7.0 (Mattigod et al. 1997). The $Ni^{2+}$ solution pH was adjusted by adding negligible volumes of 0.1 M NaOH or HCl. In nickel-containing wastewater, there are also other types of heavy metal ions such as Pb, Cu, Cd, Zn, Cr, etc. (Argun 2008; Cheung 2010; Villaescusa et al. 2004). In this study, four different metal ions ($Pb^{2+}$, $Cu^{2+}$, $Cd^{2+}$, $Zn^{2+}$) thus were chosen as the coexisting ions, whose solution concentrations were the same as that of $Ni^{2+}$.

To determine the adsorption isotherms, different concentrations of $Ni(NO_3)_2$ solutions (i.e., 10, 20, 50, 100, 150, 250, 300, 500, and 1000 mg/L) were selected to perform the adsorption experiments at (25 ± 1 °C) for 24 h. The parameters of isotherm models were used to describe the process of adsorption and adsorption mechanisms. Commonly used adsorption isotherm models such as Langmuir adsorption model (Langmuir 2015) and Freundlich adsorption model (Ng et al. 2002) were used to simulate the experimental data.

Adsorption kinetics of modified biochar was analyzed by setting different adsorption times (i.e. 0.5, 1, 2, 5, 12, 15, 20, 24, 48, 72, and 96 h), and then the adsorbed amount under different adsorption times was analyzed. The dynamics of the adsorption process was simulated by the pseudo-first-order model (Cassidy and Long 1990), pseudo-second-order model (Ho and Ofomaja 2006), and Elovich model (Shigehisa et al. 2015).

## Results and discussion

### Initial assessment

The results of adsorption capacities of biochars derived from four different raw materials in three kinds of temperature (300, 450, and 600 °C) are listed in Table 1. The results showed that CC450 had the best adsorption of $Ni^{2+}$. Then, CC450 was thus modified by 2 mol/L $Na_2S$ solution and named as MCC450.

**Table 3** Kinetic model parameters of Ni adsorption on MCC450

| Pseudo-first-order | | | Pseudo-second-order | | | Elovich model | | |
|---|---|---|---|---|---|---|---|---|
| $q_e$ (mg/g) | $k_1$ ($min^{-1}$) | $R^2$ | $q_e$ (mg/g) | $k_2$ (g/mg $min^{-1}$) | $R^2$ | $\alpha$ | $\beta$ | $R^2$ |
| 16.10 | 0.0395 | 0.941 | 20.40 | 0.0019 | 0.947 | 1.176 | 0.193 | 0.955 |

## Adsorption isotherms and kinetics

MCC450 was selected for adsorption isotherm and kinetic experiments. Adsorption isotherms of $Ni^{2+}$ showed relatively high equilibrium concentrations (Fig. 1). The adsorption isotherm of $Ni^{2+}$ was best fitted by the Freundlich model with $R^2$ of 0.94 (Table 2). The Freundlich model is well suited to describe the adsorption behavior of adsorbate on heterogeneous surfaces. The presence of functional groups on the surface of biochar, such as –COOH and –CH, could explain the good fitting of the Freundlich model (Qi et al. 2013). The maximum sorption capacity of MCC450 to $Ni^{2+}$ was about 15.40 mg/g.

The adsorption equilibrium time of MCC450 to nickel was about 24 h (Fig. 2). After 24 h, the amount of adsorption increases slowly. Pseudo-first-order, pseudo-second-order, and Elovich models were used to simulate the sorption kinetics data (Table 3). The three models simulated the kinetics of MCC450 adsorption on $Ni^{2+}$ well. The $R^2$ values of the three models were all above 0.945.The $R^2$ value of the Elovich equation was up to 0.955. This indicates that the Elovich model results matched the kinetic data the best.

## Effects of pH, temperature, and coexisting ions

Influence of pH on the MCC450 adsorption to $Ni^{2+}$ was studied in a range of 1.8 to 7.0. Initial pH had a linear relationship with adsorption amount (Fig. 3). With the increase of pH, the adsorption capacity of MCC450 to $Ni^{2+}$ showed a rising trend. When pH was 7.0, the adsorption capacity reached a maximum of 8.59 mg/g. When pH decreased, the adsorption capacity also decreased till pH was 2.62 and the adsorption amount was only 0.21 mg/g. When the solution pH was low, the functional groups and surface charges on the biochar hampered the adsorption of heavy metal ions. As the pH increased,

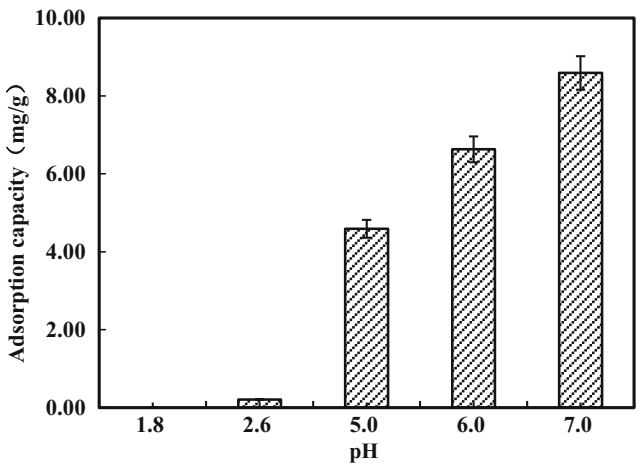


**Fig. 3** Effect of initial pH on nickel adsorption. Bars are means of triplicated data points, and error bars are the standard deviations

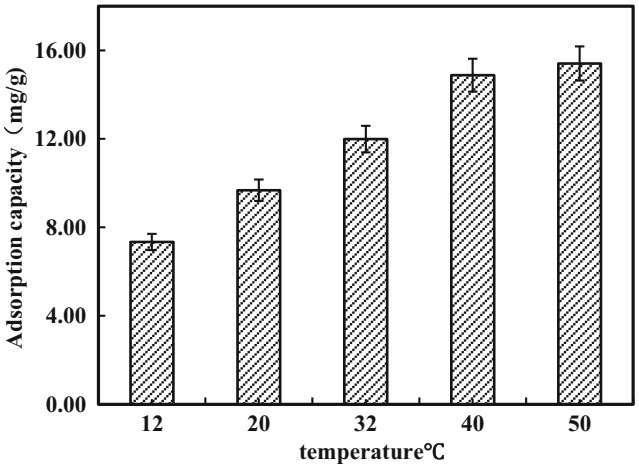


**Fig. 4** Effect of temperature on adsorption capacity. Bars are means of triplicated data points, and error bars are the standard deviations

the adsorption capacity of nickel would increase. The results were similar with the findings of a previous research that indicated that the adsorption of heavy metal ions was controlled by electrostatic interactions (Wang et al. 2015). Based on the results, pH 6 was selected as the optimal pH for further research.

The adsorption of $Ni^{2+}$ on MCC450 increased with the increase of temperature at the range of 10~50 °C (Fig. 4). When the temperatures were 12 and 50 °C, the adsorption capacities were 7.34 and 15.41 mg/g, respectively. This phenomenon showed that the adsorption process was a kind of endothermic reaction, and adsorption capacity was large at high temperature. This is consistent with the results of Mohan et al. (2011).

Mixed solutions of $Pb(NO_3)_2$, $Cd(NO_3)_2$, $Cu(NO_3)_2$, $Zn(NO_3)_2$, and $Ni(NO_3)_2$ were established with all the cation concentrations of 50 mg/L. When the five cations existed together, the nickel adsorption on MCC450 dramatically decreased and the adsorbed amount was only 1.40 mg/g (Fig. 5). The adsorption capacity of MCC450 to $Pb^{2+}$ was

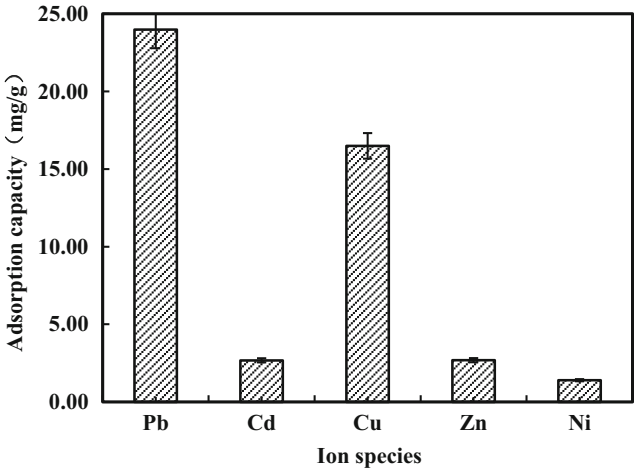


**Fig. 5** Effect of coexisting ions on nickel adsorption. Bars are means of triplicated data points, and error bars are the standard deviations

**Table 4** Specific surface area and pore volume of CC450 before and after modification

| Category | BET specific surface area ($m^2$/g) | Micropore surface areas ($m^2$/g) | External specific surface areas ($m^2$/g) | Total pore volume ($cm^3$/g) | Micropore volumes ($cm^3$/g) | Average pore diameter (nm) |
|---|---|---|---|---|---|---|
| CC450 | 11.8134 | 3.9325 | 7.8821 | 0.1197 | 0.0021 | 40.5146 |
| MCC450 | 195.6426 | 117.1078 | 78.5347 | 0.2340 | 0.0606 | 47.8510 |

the largest (23.98 mg/g), followed by $Cu^{2+}$ (16.49 mg/g). The adsorption amount of the other three ions was smaller. MCC450 adsorbed different ions simultaneously, but absorbed $Pb^{2+}$ and $Cu^{2+}$ preferentially. This led to the decrease in adsorption capacity of $Ni^{2+}$, which was similar to the findings of Xue et al. (2012).

## Physiochemical properties

### Specific surface area and pore size analysis

After modification, the BET-specific surface area of CC450 increased from 11.8134 to 195.6426 $m^2$/g. In addition, the micropore surface area increased from 3.9325 to 117.1078 $m^2$/g, and the micropore volumes increased from 0.0021 to 0.0606 $cm^3$/g. These data indicated an improvement in physical adsorption potential (Table 4).

The pores on the surface of adsorbent can be divided into macropore (50~10,000 nm), mesopore (2~50 nm), and micropore (< 2 nm). Large adsorbate can be attached to large pores (macropores and mesopores), while the micropore adsorbs small adsorbates. The micropore surface areas and micropore volumes of MCC450 were obviously increased after modification, which are beneficial for adsorption of $Ni^{2+}$. It was speculated that $Ni^{2+}$ could be removed partly by physical adsorption in micropores, but physical adsorption might not be the main removal mechanism.

### Scanning electron microscope analysis

MCC450 was regarded as an adsorbent with porous surface and developed a porous structure (Fig. 6). When the biomass was pyrolyzed, part of the organic compounds reacted to generate the volatile gaseous substance, and the porous structure was formed on the surface and inside of the adsorbent. The porous structure greatly increased the specific surface area of the biochar, which facilitated the introduction of new functional groups. In addition, the contact probability of the adsorbate in the solution and the surface adsorption sites of biochar increased. Furthermore, the adsorption performance of biochar greatly improved, which was consistent with the results of the BET analysis.

Analyzing the data of SEM and BET characterization before and after modification suggested that the specific surface area and micropore surface area increased by 16 and 29 times, respectively, after modification. As a result, the amount of adsorption only increased from 7.85 to 15.40 mg/g. These suggested that the surface functional groups might have a major effect in the adsorption process.

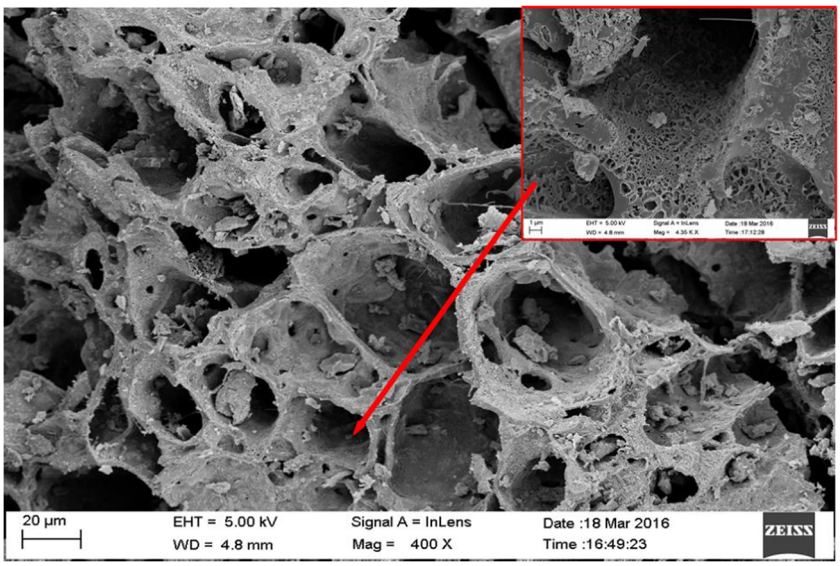


**Fig. 6** SEM analysis of MCC450

### Surface functional group analysis

There are different vibration modes among different functional groups, such as stretching, rotation, symmetry, and asymmetry. This makes different functional groups have different peak values (peak or trough) in the infrared absorption spectrum. FTIR scanning was performed for CC450 and of MCC450 before and after adsorption (Fig. 7).

In the FTIR spectra of the biochar before and after modification, the carbonyl (C=O) had a peak at around 1585~1614 $cm^{-1}$ (Yorgun and Yıldız 2015). The carbon oxygen bonds (C–O, C–O–C) (peaks at 1106~1110 $cm^{-1}$) and carboxyl (–COOH) (a peak near 1380 $cm^{-1}$) (Frišták et al. 2017) were enhanced, which was caused by the introduction of modifier. Abdelouahab-Reddam et al. (A Sepúlveda-Escribano 2014) impregnated activated carbon with sodium sulfide solution and sulfuric acid at low 25 °C. Their results showed that thiol-type sulfur compounds (R-SH) were formed on the surface of activated carbon, and the oxygen content increased simultaneously.

A weak vibration band was added at 1164 $cm^{-1}$ in the modified biochar spectra. It was found in the literature that the peak should be the band of sulfoxide (–SO–) (Seredych and Bandosz 2011). This is consistent with the results of XPS; after modification, some of the original oxygen functional groups in biochar are decomposed under the condition of high temperature of 450 °C.

The absorption peak at 1382.7 $cm^{-1}$ was markedly increased in MCC450 spectra after adsorption. Based on previous results, this peak was the result of metal carboxylate (–COO) (Ibrahim and Jalbout 2008), which proved that metal ions interacted with organic functional groups during adsorption.

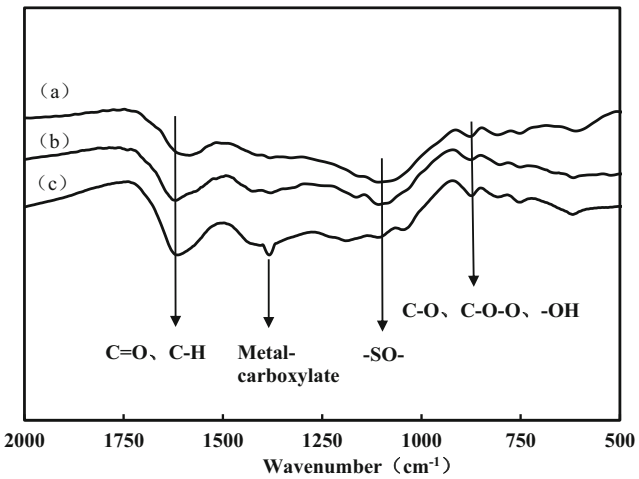


**Fig. 7** FTIR of CC450 (**a**) and MCC450 before (**b**) and after (**c**) adsorption

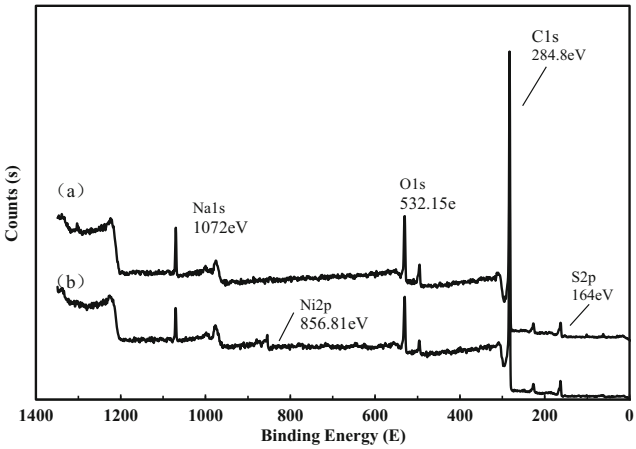


**Fig. 8** XPS full spectrum scan of MCC450 before and after adsorption

### X-ray photoelectron spectroscopic analysis

According to the spectrum of XPS scanning (Fig. 8), the basic elements of biochar were as follows: C element of 85.12%, N element of 0.6%, O element of 10.47%, and S element of 3.81%. The Ni element was not detected in the original sample. After adsorption, the basic elements of biochar were C of 83.28%, N of 0.52%, O of 10.73%, S of 4.6%, and nickel of 0.88% (Table 5). After the adsorption, the nickel element increased obviously, indicating that the nickel was adsorbed on the biochar surface.

High-resolution XPS spectra show that C1s (Fig. 9a) had three peaks, and the corresponding binding energies were 284.8, 286.0, and 289.0 eV, respectively. According to the XPS database of Thermo Scientific, the corresponding functional groups were C–C, glycosidic bond (C–O–C), and ester groups (–COO) (Olayo et al. 2016). Three peaks were observed from the high-resolution spectra of O1s (Fig. 9b).The binding energy peak at 531.5 eV can be assigned to the organic C–O functional group and, at 532.9 eV, can be assigned to the organic C=O functional group. The weak peak at 536.5 eV is corresponding to C–O (Skryleva et al. 2016).

Figure 9c shows the sulfur high-resolution XPS spectra of MCC450. The presence of a peak at 163.9 eV can be related to the sulfhydryl group (–SH) (Guan et al. 2017; Sohn and Park 2003), which is consistent with the result of FTIR. A weak peak observed at 165.1 eV is associated with the S–C key according to the NIST X-ray Photoelectron Spectroscopy

**Table 5** Content of each element in MCC450 before and after adsorption

| MCC450 | C/% | O/% | N/% | S/% | Ni/% |
|---|---|---|---|---|---|
| Before adsorption | 85.12 | 10.47 | 0.6 | 3.81 | – |
| After adsorption | 83.28 | 10.73 | 0.52 | 4.6 | 0.88 |

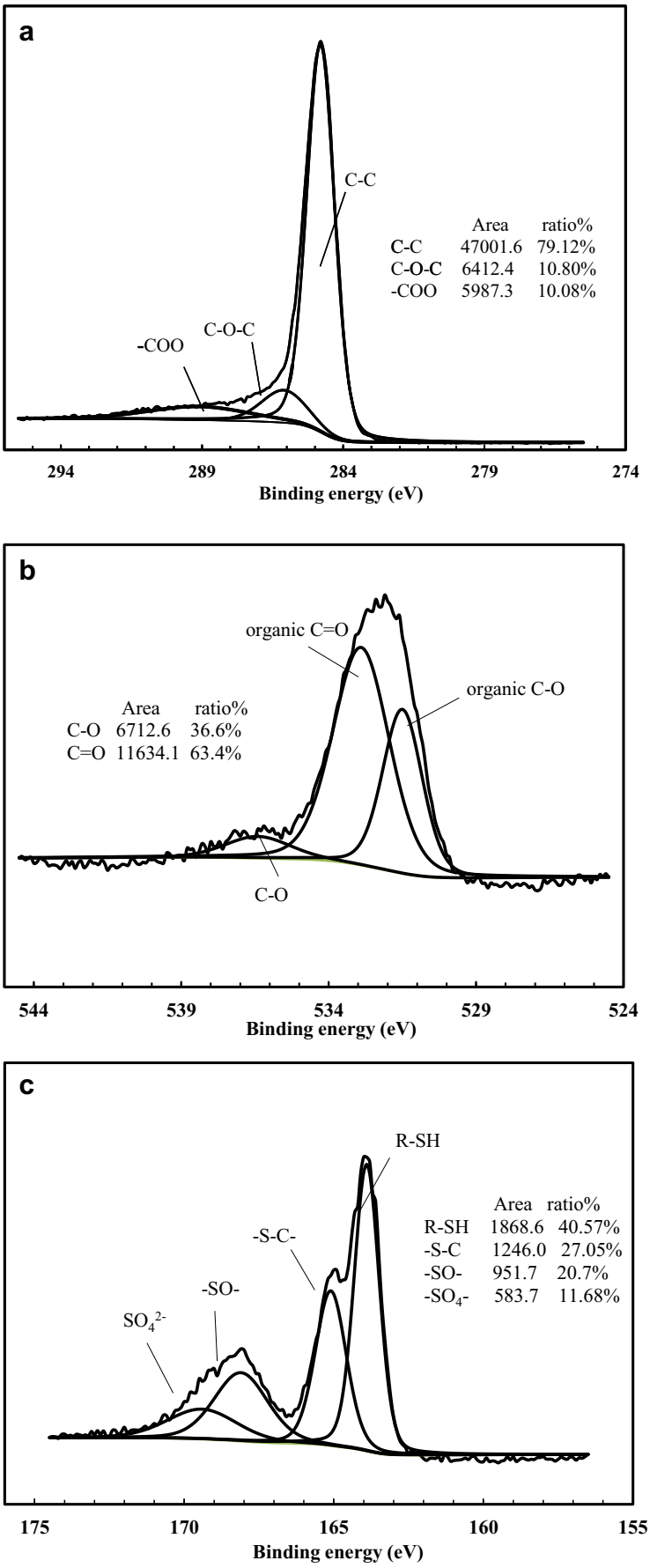


**Fig. 9** High-resolution XPS of C1s (**a**), O1s (**b**), and S2p (**c**) before adsorption

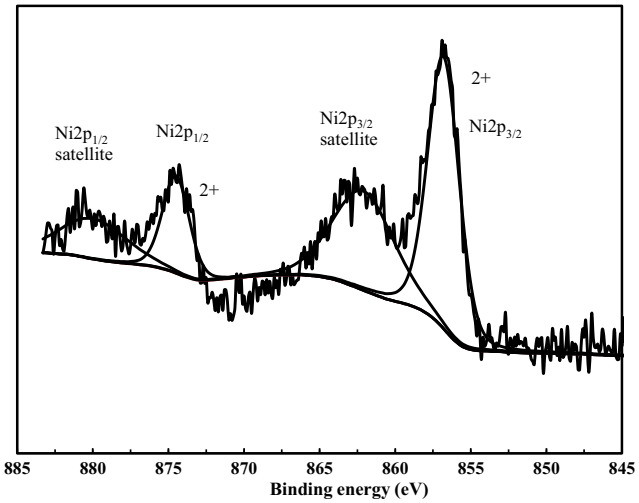


**Fig. 10** High-resolution XPS of Ni2p after adsorption

Database. The peaks at 168.1 and 169.4 eV may be caused by the surface oxidation of S (Maciel et al. 2010), which can be linked to –SO– and $–SO_4–$.

The Ni2p spectrum (Fig. 10) after adsorption exhibited two contributions, 2p1/2 and 2p3/2, located at respectively 856.8 and 874.5 eV with their satellite peaks indicating that the position of the peaks related to $Ni^{2+}$ (Guan et al. 2017; Sohn and Park 2003).

In the experiment of three influencing factors, ion exchange might be the main adsorption mechanism. XPS and FTIR proved that the presence of some functional groups in biochar affected the adsorption processes, such as carboxyl and sulfhydryl groups.

The adsorption process thus can be assumed to be as follows:

$$2{-}COOH + Ni^{2+} \leftrightarrow {-}COO{-}Ni^{+} + H^{+} \quad (3.1)$$

$$-SH + Ni^{2+} \leftrightarrow -R{-}S{-}Ni^{+} + H^{+} \quad (3.2)$$

It was speculated that there were two mechanisms controlling MCC450 adsorption of nickel–ion exchange and physical adsorption. The specific surface area and pore structure of MCC450 developed greatly after modification, which resulted in high adsorption properties. On the other hand, $Ni^{2+}$ exchanged with $H^+$ in –COOH and –SH, then was adsorbed onto the surface.

## Conclusions

MCC450 was produced by modifying CC450 biochar with 2 mol/L $Na_2S$ to remove nickel from water. The nickel adsorption kinetics of MCC450 followed the Elovich model with the equilibrium time of 24 h. The maximum nickel adsorption capacity of MCC450 was 15.40 mg/g. Temperature, pH, and coexisting ions strongly affected the adsorption of nickel on MCC450. Findings from the characterization experiments showed that the main adsorption mechanisms of $Ni^{2+}$ on MCC450 were ion exchange and physical adsorption. This work indicates that biochar has huge potential to be used as alternative adsorbent for the removal of nickel from wastewater.

**Acknowledgements** This work was partially supported by the National "Twelfth Five-Year" Plan for the Science & Technology Pillar Program (grant numbers 2014BAL04B04 and 2015BAL01B02), the Fundamental Research Funds for the Central Universities (no. 2042016kf0173), and the Wuhan Water Engineering & Technology Co., Ltd. The authors also thank the anonymous reviewers for their invaluable insight and helpful suggestions.

## References

Akhtar N, Iqbal J, Iqbal M (2004) Removal and recovery of nickel(II) from aqueous solution by loofa sponge-immobilized biomass of Chlorella sorokiniana : characterization studies. J Hazard Mater 108:85–94

Alvarez-Ayuso E, Garcia-Sanchez A, Querol X (2003) Purification of metal electroplating waste waters using zeolites. Water Res 37(20): 4855–4862. https://doi.org/10.1016/j.watres.2003.08.009

Alyüz B, Veli S (2009) Kinetics and equilibrium studies for the removal of nickel and zinc from aqueous solutions by ion exchange resins. J Hazard Mater 167(1-3):482–488. https://doi.org/10.1016/j.jhazmat.2009.01.006

Argun ME (2008) Use of clinoptilolite for the removal of nickel ions from water: kinetics and thermodynamics. J Hazard Mater 150(3):587–595. https://doi.org/10.1016/j.jhazmat.2007.05.008

Banerjee SS, Jayaram RV, Joshi MV (2003) Removal of nickel(II) and zinc(II) from wastewater using fly ash and impregnated fly ash. Sep Sci Technol 38(5):1015–1032. https://doi.org/10.1081/SS-120018121

Cassidy JF, Long C (1990) Mathematical model for the measurement of pseudo-first-order rate constants in laser flash photolysis experiments. J Photochem Photobiol A Chem 54:1–10

Cheung PCP (2010) Nickel structures and methods for manufacturing the same by removal of an underlying material. US

Christensen ER, Delwiche JT (1982) Removal of heavy metals from electroplating rinsewaters by precipitation, flocculation and ultrafiltration. Water Res 16(5):729–737. https://doi.org/10.1016/0043-1354(82)90098-7

Ding Z, Hu X, Wan Y, Wang S, Gao B (2016) Removal of lead, copper, cadmium, zinc, and nickel from aqueous solutions by alkali-modified biochar: batch and column tests. J Ind Eng Chem 33: 239–245. https://doi.org/10.1016/j.jiec.2015.10.007

Doumer ME, Rigol A, Vidal M, Mangrich AS (2016) Removal of Cd, Cu, Pb, and Zn from aqueous solutions by biochars. Environ Sci Pollut Res 23(3):2684–2692. https://doi.org/10.1007/s11356-015-5486-3

Frišták V, Víglašová E, Ďuriška L, Galamboš M, Moreno-Jimenéz E, Pipíška M, Soja G (2017) Sorption separation of Eu and As from single-component systems by Fe-modified biochar: kinetic and equilibrium study. J Iran Chem Soc 14:521–530

Goel J, Kadirvelu K, Rajagopal C, Garg VK (2005) Investigation of adsorption of lead, mercury and nickel from aqueous solutions onto carbon aerogel. J Chem Technol Biotechnol 80(4):469–476. https://doi.org/10.1002/jctb.1212

Guan B, Li Y, Yin B, Liu K, Wang D, Zhang H, Cheng C (2017) Synthesis of hierarchical NiS microflowers for high performance asymmetric supercapacitor. Chem Eng J 308:1165–1173

Gupta VK, Jain CK, Ali I, Sharma M, Saini VK (2003) Removal of cadmium and nickel from wastewater using bagasse fly ash—a sugar industry waste. Sep Sci 37:4038–4044

Higashikawa FS, Conz RF, Colzato M, Cerri CEP, Alleoni LRF (2016) Effects of feedstock type and slow pyrolysis temperature in the production of biochars on the removal of cadmium and nickel from water. J Clean Prod 137:965–972. https://doi.org/10.1016/j.jclepro.2016.07.205

Ho YS, Ofomaja AE (2006) Pseudo-second-order model for lead ion sorption from aqueous solutions onto palm kernel fiber. J Hazard Mater 129(1-3):137–142. https://doi.org/10.1016/j.jhazmat.2005.08.020

Ibrahim AHM, Jalbout A (2008) Molecular spectroscopic study of River Nile sediment in the greater Cairo region. Appl Spectrosc 62(3):306–311. https://doi.org/10.1366/000370208783759795

Ismail I, Soliman A, Abdel-Monem N, Ahmed HS, Sorour MH (2014) Nickel removal from electroplating waste water using stand-alone and electrically assisted ion exchange processes. Int J Environ Sci Technol 11(1):199–206. https://doi.org/10.1007/s13762-012-0158-z

Kobya M, Demirbas E, Senturk E, Ince M (2005) Adsorption of heavy metal ions from aqueous solutions by activated carbon prepared from apricot stone. Bioresour Technol 96(13):1518–1521. https://doi.org/10.1016/j.biortech.2004.12.005

Langmuir I (2015) The adsorption of gases on plane surfaces of glass, mica and platinum. J Chem Phys 40:1361–1403

Liu ZG, Zhang FS (2009) Removal of lead from water using biochars prepared from hydrothermal liquefaction of biomass. J Hazard Mater 167(1-3):933–939. https://doi.org/10.1016/j.jhazmat.2009.01.085

Long L, Xue Y, Zeng Y, Yang K, Lin C (2017) Synthesis, characterization and mechanism analysis of modified crayfish shell biochar possessed ZnO nanoparticles to remove trichloroacetic acid. J Clean Prod 166

Maciel J, Martins MC, Barbosa MA (2010) The stability of self-assembled monolayers with time and under biological conditions. J Biomed Mater Res A 94:833–843. https://doi.org/10.1002/jbm.a.32746

Mansoorian HJ, Rajabizadeh A, Bazrafshan E, Mahvi AH (2012) Practical assessment of electrocoagulation process in removing nickel metal from aqueous solutions using iron-rod electrodes. Desalin Water Treat 44(1-3):29–35. https://doi.org/10.1080/19443994.2012.691708

Mattigod SV, Rai D, Felmy AR, Rao L (1997) Solubility and solubility product of crystalline Ni(OH) 2. J Solut Chem 26(4):391–403. https://doi.org/10.1007/BF02767678

Mohan D, Rajput S, Singh VK, Steele PH, Pittman CU (2011) Modeling and evaluation of chromium remediation from water using low cost biochar, a green adsorbent. J Hazard Mater 188(1-3):319–333. https://doi.org/10.1016/j.jhazmat.2011.01.127

Mohan D, Sarswat A, Ok YS, Jr PC (2014) Organic and inorganic contaminants removal from water with biochar, a renewable, low cost and sustainable adsorbent—a critical review. Bioresour Technol 160:191–202. https://doi.org/10.1016/j.biortech.2014.01.120

Mosa A, El-Banna MF, Gao B (2016) Biochar filters reduced the toxic effects of nickel on tomato (Lycopersicon esculentum L.) grown in nutrient film technique hydroponic system. Chemosphere 149:254–262. https://doi.org/10.1016/j.chemosphere.2016.01.104

Ng C, Losso JN, Marshall WE, Rao RM (2002) Freundlich adsorption isotherms of agricultural by-product-based powdered activated carbons in a geosmin-water system. Bioresour Technol 85(2):131–135. https://doi.org/10.1016/s0960-8524(02)00093-7

Olayo MG, Zúñiga R, González-Salgado F, Gómez LM, González-Torres M, Basurto R, Cruz GJ (2016) Structure and morphology of plasma polyfuran particles. Polym Bull 74(2):571–581. https://doi.org/10.1007/s00289-016-1730-3

Qi X, Li L, Tan T, Chen W, Jr SR (2013) Adsorption of 1-butyl-3-methylimidazolium chloride ionic liquid by functional carbon microspheres from hydrothermal carbonization of cellulose. Environ Sci Technol 47(6):2792–2798. https://doi.org/10.1021/es304873t

Rosengren Å, Pavlovic E, Oscarsson S, Krajewski A, Ravaglioli A, Piancastelli A (2002) Plasma protein adsorption pattern on characterized ceramic biomaterials. Biomaterials 23(4):1237–1247. https://doi.org/10.1016/S0142-9612(01)00244-7

Sandau E, Sandau P, Pulz O (2010) Heavy metal sorption by microalgae. Acta Biotechnol 16:227–235

Sepúlveda-Escribano ZA-e A, Wahby A, Silvestre-Albero J, Rodríguez-Reinoso F (2014) Activated carbons impregnated with Na2S and H2SO4 texture, surface chemistry and application to mercury removal from aqueous solutions. Adsorpt Sci Technol 32:101

Seredych M, Bandosz TJ (2011) Removal of dibenzothiophenes from model diesel fuel on sulfur rich activated carbons. Appl Catal B Environ 106:133–141

Shigehisa T, Inoue T, Kumagai H (2015) Mathematical model of the water sorption kinetics of UBC. Fuel Process Technol 137:194–203

Shukla SS, Li JY, Dorris KL, Shukla A (2005) Removal of nickel from aqueous solutions by sawdust. J Hazard Mater 121(1-3):243–246. https://doi.org/10.1016/j.jhazmat.2004.11.025

Skryleva EA, Kubasov IV, Kiryukhantsev-Korneev PV, Senatulin BR, Zhukov RN, Zakutailov KV, Malinkovich MD, Parkhomenko YN (2016) XPS study of Li/Nb ratio in LiNbO 3 crystals. Effect of polarity and mechanical processing on LiNbO 3 surface chemical composition. Appl Surf Sci 389:387–394. https://doi.org/10.1016/j.apsusc.2016.07.108

Sohn JR, Park WC (2003) The roles of active sites of nickel sulfate supported on gamma-Al2O3 for ethylene dimerization. Appl Catal A Gen 239(1-2):269–278. https://doi.org/10.1016/S0926-860X(02)00392-7

Vaughan T, Seo CW, Marshall WE (2001) Removal of selected metal ions from aqueous solution using modified corncobs. Bioresour Technol 78(2):133–139. https://doi.org/10.1016/S0960-8524(01)00007-4

Villaescusa I, Fiol N, Martínez M, Miralles N, Poch J, Serarols J (2004) Removal of copper and nickel ions from aqueous solutions by grape stalks wastes. Water Res 38(4):992–1002. https://doi.org/10.1016/j.watres.2003.10.040

Wang DC, Xia ZZ, Wu JY, Wang RZ, Zhai H, Dou WD (2005) Study of a novel silica gel–water adsorption chiller. Part I. Design and performance prediction. Int J Refrig 28(7):1073–1083. https://doi.org/10.1016/j.ijrefrig.2005.03.001

Wang H, Gao B, Wang S, Fang J, Xue Y, Yang K (2015) Removal of Pb(II), Cu(II), and Cd(II) from aqueous solutions by biochar derived from KMnO4 treated hickory wood. Bioresour Technol 197:356–362. https://doi.org/10.1016/j.biortech.2015.08.132

Xu Y, Zhao D (2007) Reductive immobilization of chromate in water and soil using stabilized iron nanoparticles. Water Res 41(10):2101–2108. https://doi.org/10.1016/j.watres.2007.02.037

Xue YW, Gao B, Yao Y, Inyang M, Zhang M, Zimmerman AR, Ro KS (2012) Hydrogen peroxide modification enhances the ability of biochar (hydrochar) produced from hydrothermal carbonization of peanut hull to remove aqueous heavy metals: batch and column tests. Chem Eng J 200:673–680. https://doi.org/10.1016/j.cej.2012.06.116

Yavuz O, Altunkaynak Y, Guzel F (2003) Removal of copper, nickel, cobalt and manganese from aqueous solution by kaolinite. Water Res 37(4):948–952. https://doi.org/10.1016/s0043-1354(02)00409-8

Yorgun S, Yıldız D (2015) Preparation and characterization of activated carbons from Paulownia wood by chemical activation with H3PO4. J Taiwan Inst Chem Eng 53:122–131. https://doi.org/10.1016/j.jtice.2015.02.032